

Oxidation resistance of (Ti,Al,Cr)N coatings at 800 °C

LI Ming-sheng (李明升)¹, FENG Chang-jie(冯长杰)², YANG Gan-lan(杨干兰)¹,
HE Xiang-ming(何向明)¹, LI Wen-kui(李文魁)¹, XIANG Jun-huai(向军淮)¹

1. Jiangxi Key Laboratory of Surface Engineering, Jiangxi Science and Technology Normal University,
Nanchang 330013, China;
2. Department of Materials Science and Engineering, Nanchang Institute of Aeronautical Technology,
Nanchang 330063, China

Received 15 July 2007; accepted 10 September 2007

Abstract: The composite metastable $(\text{Ti}_{0.5}\text{Al}_{0.5})\text{N}$, $(\text{Ti}_{0.45}\text{Al}_{0.45}\text{Cr}_{0.1})\text{N}$ and $(\text{Ti}_{0.35}\text{Al}_{0.35}\text{Cr}_{0.3})\text{N}$ coatings were respectively deposited on a wrought martensite steel 1Cr11Ni2W2MoV for aero-engine compressor blades by arc ion plating technique with pulse substrate bias. All the coatings have B1NaCl phase with a (200) preferred orientation and dense structures. The results show that the introduction of Cr into (Ti,Al)N gives rise to a minute shrinkage of crystal lattice. The incorporation of chromium into the coatings dramatically improves the oxidation-resistance of the coatings. For $(\text{Ti}_{0.5}\text{Al}_{0.5})\text{N}$, a layered oxide scale forms after 100 h oxidation and the outer layer is the blend oxide of TiO_2 and Al_2O_3 , and the middle layer is rich in Al and the inner layer is rich in Ti. For $(\text{Ti}_{0.45}\text{Al}_{0.45}\text{Cr}_{0.1})\text{N}$, the oxide scale possesses a double-layered structure and the outer layer is rich in Ti. For $(\text{Ti}_{0.35}\text{Al}_{0.35}\text{Cr}_{0.3})\text{N}$, a Cr-rich compound oxide scale of Ti, Al and Cr forms, and a out-diffusion of Fe from steel to the nitride coating and oxide film during the oxidation takes place.

Key words: (Ti,Al,Cr)N; oxidation resistance; arc ion plating

1 Introduction

Titanium nitride (TiN) coating is extensively used to increase the lifetime of cutting and forming tools due to its high mechanical hardness and low friction coefficient[1-3]. But TiN can be oxidized rapidly in air at temperatures above 550 °C [4]. Titanium aluminum nitride ternary solid solution coating of B1NaCl structure has been successfully developed as an alternative coating material for more than 10 years due to its superior oxidation-resistance and mechanical properties[5-7]. At 800 °C, the $(\text{Ti}_{0.5}\text{Al}_{0.5})\text{N}$ coating can provide protection for the substrate for up to 100 h[8]. Since the (Ti,Al)N coating possesses higher hardness and more excellent oxidation-resistance than TiN, it can be used not only as hard coating for cutting and forming tools, but also as protective coating for stainless steel and titanium alloy. In order to improve the mechanical property and oxidation-resistance of the (Ti,Al)N coating, some

researchers have attempted to add the third metal element such as yttrium[8-9], chromium[10] and niobium[11] into the coating, and some significant results have been presented. But systematical research is still inadequate up to now. In this study, the composite metastable $(\text{Ti}_{0.5}\text{Al}_{0.5})\text{N}$, $(\text{Ti}_{0.45}\text{Al}_{0.45}\text{Cr}_{0.1})\text{N}$ and $(\text{Ti}_{0.35}\text{Al}_{0.35}\text{Cr}_{0.3})\text{N}$ coatings were respectively deposited on a wrought martensite steel 1Cr11Ni2W2MoV for aero-engine compressor blades by arc ion plating with a pulse bias. The structure and oxidation-resistance of the coatings at 800 °C was investigated.

2 Experimental

The nitride compound coatings were respectively deposited on 1Cr11Ni2W2MoV stainless steel sheets (15 mm×10 mm×2 mm) by AIP-1000-10 Coating System. The steel sheets were prepared by mirror-polishing, followed by ultrasonic cleaning in alcohol and acetone solution, and were sputter-cleaned using Ar ion under

Foundation item: Project (50401022) supported by the National Natural Science Foundation of China; Project (0650034) supported by the Natural Science Foundation of Jiangxi Province, China

Corresponding author: LI Ming-sheng; Tel: +86-791-3831266; E-mail:mshli@163.com

-1 000 V (DC) bias voltage to remove contaminant layer. $(\text{Ti}_{0.5}\text{Al}_{0.5})\text{N}$ coatings were deposited by using a single $\text{Ti}_{0.5}\text{Al}_{0.5}$ evaporator. $(\text{Ti}_{0.45}\text{Al}_{0.45}\text{Cr}_{0.1})\text{N}$ and $(\text{Ti}_{0.35}\text{Al}_{0.35}\text{Cr}_{0.3})\text{N}$ were prepared by a two-source mode, in which one evaporator was fitted with a chromium cathode and the other with an $(\text{Ti}_{0.5}\text{Al}_{0.5})$ alloy cathode. By controlling the currents of two evaporators and adjusting the position of the substrates, $(\text{Ti},\text{Al},\text{Cr})\text{N}$ of different metal composition was acquired. The process parameters were listed as follows: deposition temperature of 400 °C, total pressure of 1.2 Pa, N_2 partial pressure of 0.8 Pa, arc voltage of 20 V, arc current of 40–100 A, pulse bias voltage of -600 V, duty cycle of 20% and frequency of 20 kHz.

The structural phases of the coatings were characterized by XRD with Cu K_α radiation. The oxidation was carried out in a chamber-type electric furnace at 800 °C for 100 h in air. The oxide scale was examined using a field emission SEM with EDS.

3 Results and discussion

The chemical composition of metal elements in the as-deposited coatings was measured by EPMA and the chemical formula of the coatings can be approximatively described as $(\text{Ti}_{0.5}\text{Al}_{0.5})\text{N}$, $(\text{Ti}_{0.45}\text{Al}_{0.45}\text{Cr}_{0.1})\text{N}$ and $(\text{Ti}_{0.35}\text{Al}_{0.35}\text{Cr}_{0.3})\text{N}$. The SEM micrographs of the coatings surfaces are shown in Fig.1. All coatings possess a dense structure and are free of pinholes. The droplets of dimension smaller than 1 μm exist in all coatings. The big droplets adhere on the surface of the coatings, only small ones are imbedded in the coatings. During the deposition of the coatings, most of the droplets are resputtered off from the coating. The XRD patterns of the as-deposited coatings are shown in Fig.2. All the coatings have $\text{B}1\text{NaCl}$ phase structure and (220) is the preferred orientation. The position of the peaks shifts to higher angles and the FWHM increases from 1° to 1.6° with increasing Cr content. Thus the introduction of chromium into $(\text{Ti},\text{Al})\text{N}$ gives rise to a minor shrinkage of crystal lattice and decreases of the grain size.

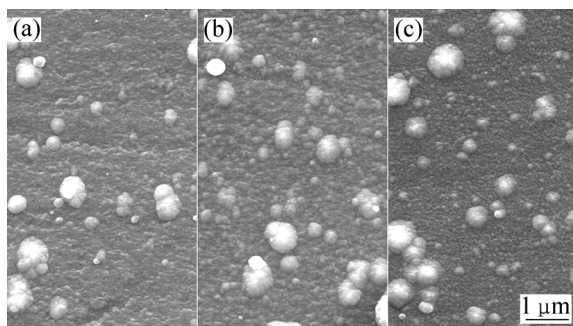


Fig.1 Surface morphologies of as-deposited coatings: (a) $(\text{Ti}_{0.5}\text{Al}_{0.5})\text{N}$; (b) $(\text{Ti}_{0.45}\text{Al}_{0.45}\text{Cr}_{0.1})\text{N}$; (c) $(\text{Ti}_{0.35}\text{Al}_{0.35}\text{Cr}_{0.3})\text{N}$

Fig.3 shows the surface morphologies of $(\text{Ti}_{0.5}\text{Al}_{0.5})\text{N}$, $(\text{Ti}_{0.45}\text{Al}_{0.45}\text{Cr}_{0.1})\text{N}$ and $(\text{Ti}_{0.35}\text{Al}_{0.35}\text{Cr}_{0.3})\text{N}$ coatings oxidized at 800 °C for 100 h. On the surface of

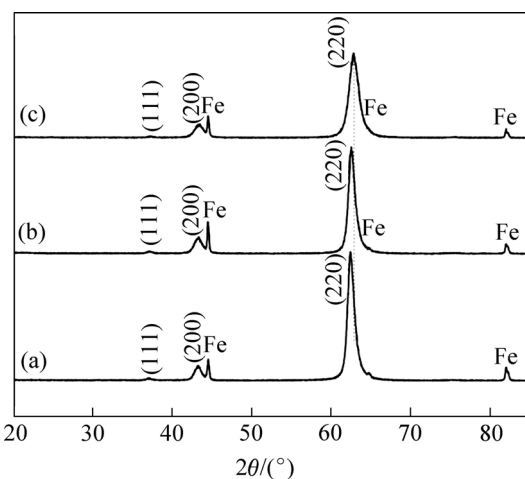


Fig.2 XRD patterns of as-deposited coatings: (a) $(\text{Ti}_{0.5}\text{Al}_{0.5})\text{N}$; (b) $(\text{Ti}_{0.45}\text{Al}_{0.45}\text{Cr}_{0.1})\text{N}$; (c) $(\text{Ti}_{0.35}\text{Al}_{0.35}\text{Cr}_{0.3})\text{N}$

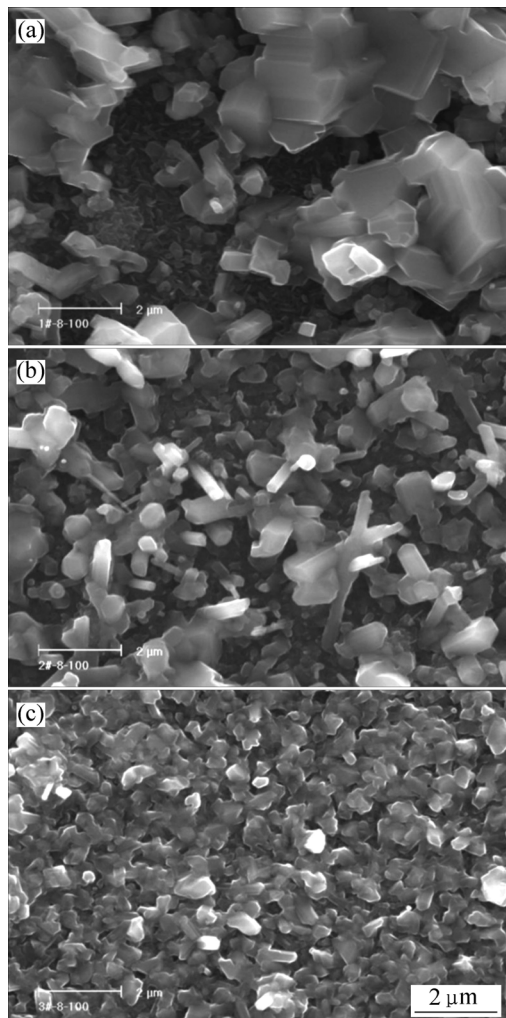


Fig.3 Surface morphologies of $(\text{Ti}_{0.5}\text{Al}_{0.5})\text{N}$ (a), $(\text{Ti}_{0.45}\text{Al}_{0.45}\text{Cr}_{0.1})\text{N}$ (b) and $(\text{Ti}_{0.35}\text{Al}_{0.35}\text{Cr}_{0.3})\text{N}$ (c) coatings oxidized at 800 °C for 100 h

$(\text{Ti}_{0.5}\text{Al}_{0.5})\text{N}$ and $(\text{Ti}_{0.45}\text{Al}_{0.45}\text{Cr}_{0.1})\text{N}$, two types of oxides can be identified, one is made up of fine crystals and the other is protruded bulky crystals. And the Al content in the fine oxide crystals is higher than that in the coarse crystals. While for $(\text{Ti}_{0.45}\text{Al}_{0.45}\text{Cr}_{0.1})\text{N}$ coating, the uniform oxide crystal forms.

The cross sectional microstructures of the oxidized specimens are shown in Fig.4 and the elemental contents of different spots marked in Fig.4 are shown in Fig.5. For $(\text{Ti}_{0.5}\text{Al}_{0.5})\text{N}$, a layered oxide scale forms after 100 h oxidation and the outer layer is the blend of Al_2O_3 and TiO_2 , and the middle layer is rich in Al and the inner layer is rich in Ti. The thickness of the oxide scale is approximately 7 μm . The oxide scale of $(\text{Ti}_{0.45}\text{Al}_{0.45}\text{Cr}_{0.1})\text{N}$ possesses a double-layered structure. Both layers are made of blend of Al_2O_3 , Cr_2O_3 and TiO_2 . But the content of Ti in outer layer is higher than that in inner one. The thickness of the oxide scale is about 2 μm . No layered structure appears in oxide film for $(\text{Ti}_{0.35}\text{Al}_{0.35}\text{Cr}_{0.3})\text{N}$ coating and Cr-riched blend oxide of

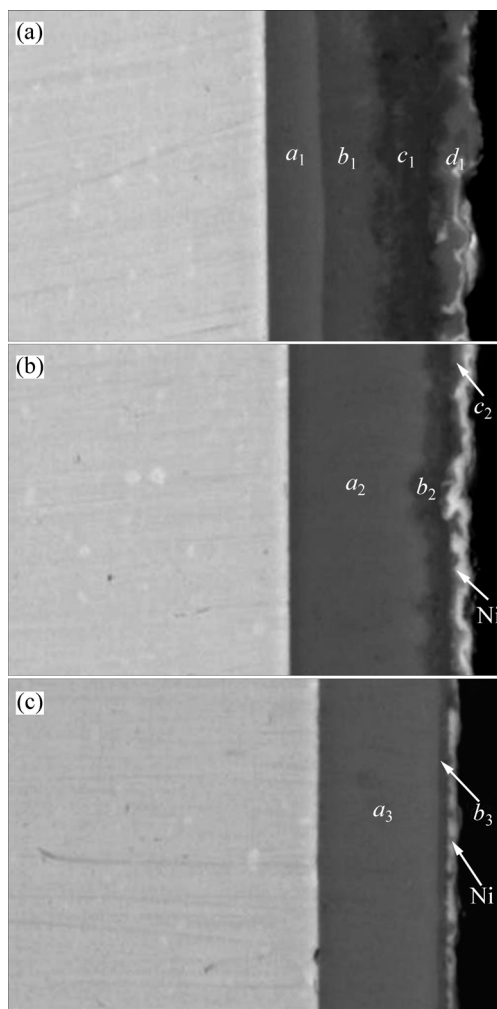


Fig.4 Cross-sectional microstructures of $(\text{Ti}_{0.5}\text{Al}_{0.5})\text{N}$ (a), $(\text{Ti}_{0.45}\text{Al}_{0.45}\text{Cr}_{0.1})\text{N}$ (b) and $(\text{Ti}_{0.35}\text{Al}_{0.35}\text{Cr}_{0.3})\text{N}$ (c) coatings oxidized at 800 $^{\circ}\text{C}$ for 100 h

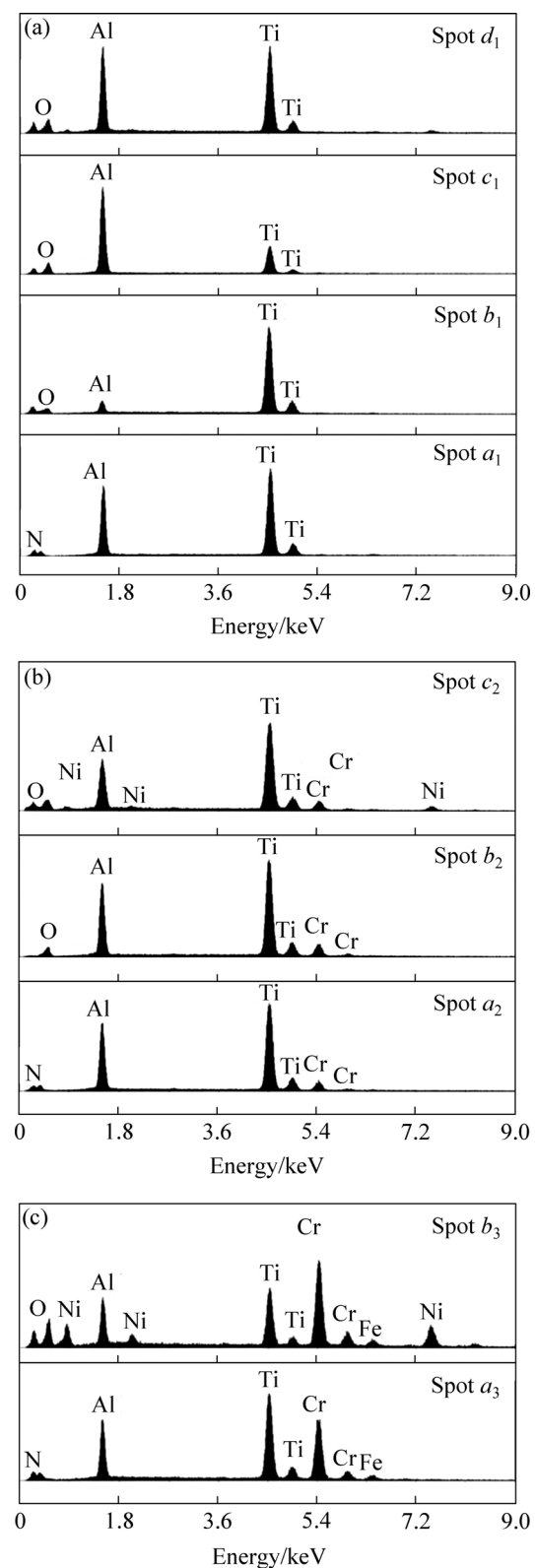


Fig.5 EDS patterns of different areas of cross-sectional morphologies shown in Fig.4 for stainless steel coated with $(\text{Ti}_{0.5}\text{Al}_{0.5})\text{N}$ (a), $(\text{Ti}_{0.45}\text{Al}_{0.45}\text{Cr}_{0.1})\text{N}$ (b) or $(\text{Ti}_{0.35}\text{Al}_{0.35}\text{Cr}_{0.3})\text{N}$ (c) after oxidation at 800 $^{\circ}\text{C}$ for 100 h

Al_2O_3 , Cr_2O_3 and TiO_2 form. The thickness of the oxide film is less than 1 μm . It is revealed by the EDS analysis

that a out-diffusion of Fe from steel to the nitride coating and oxide film takes place during the oxidation of the specimens coated with $(\text{Ti}_{0.35}\text{Al}_{0.35}\text{Cr}_{0.3})\text{N}$. And this phenomenon does not occur during the oxidation of the specimens coated with $(\text{Ti}_{0.5}\text{Al}_{0.5})\text{N}$ or $(\text{Ti}_{0.45}\text{Al}_{0.45}\text{Cr}_{0.1})\text{N}$. The incorporation of Cr into the coatings prevents the formation of the layered structure of oxide scale and dramatically decreases the oxidation rate of the nitride coatings.

It is revealed by the XRD patterns that (Fig.6) with the increase of Cr content in the coatings, the intensity of the peaks of the nitrides has a smaller change while the intensity of the diffraction peaks of oxides decreases obviously after 100 h oxidation at 800 °C. For $(\text{Ti}_{0.5}\text{Al}_{0.5})\text{N}$, rutile TiO_2 and $\alpha\text{-Al}_2\text{O}_3$ form. For $(\text{Ti}_{0.45}\text{Al}_{0.45}\text{Cr}_{0.1})\text{N}$ and $(\text{Ti}_{0.35}\text{Al}_{0.35}\text{Cr}_{0.3})\text{N}$, rutile TiO_2 , $\alpha\text{-Al}_2\text{O}_3$ and $\alpha\text{-Cr}_2\text{O}_3$ form. Since $\alpha\text{-Al}_2\text{O}_3$ and $\alpha\text{-Cr}_2\text{O}_3$ have the same phase structure and close crystal parameter, they can not be distinguished in the XRD patterns.

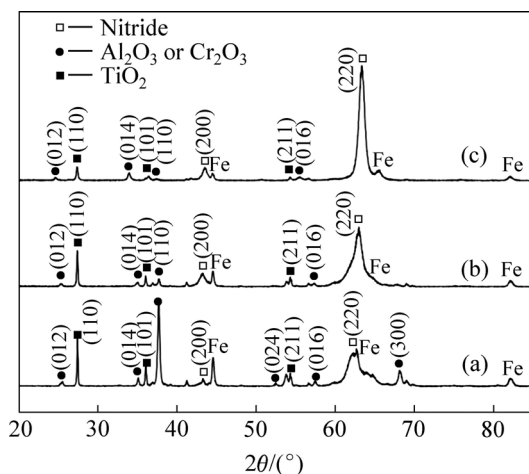


Fig.6 XRD patterns of $(\text{Ti}_{0.5}\text{Al}_{0.5})\text{N}$ (a), $(\text{Ti}_{0.45}\text{Al}_{0.45}\text{Cr}_{0.1})\text{N}$ (b) and $(\text{Ti}_{0.35}\text{Al}_{0.35}\text{Cr}_{0.3})\text{N}$ (c) coatings oxidized at 800 °C for 100 h

4 Conclusions

1) Metastable $(\text{Ti}_{0.5}\text{Al}_{0.5})\text{N}$, $(\text{Ti}_{0.45}\text{Al}_{0.45}\text{Cr}_{0.1})\text{N}$ and $(\text{Ti}_{0.35}\text{Al}_{0.35}\text{Cr}_{0.3})\text{N}$ coatings were respectively deposited on steel 1Cr11Ni2W2MoV by arc ion plating technique. All as-deposited nitride coatings have $\text{B}1\text{NaCl}$ phase and

dense structures.

2) The incorporation of Cr into the coatings prevents the formation of the layered structure of oxide scale and dramatically improves the oxidation-resistance of the nitride coatings.

References

- [1] SCHULZ A, STOCK H R, MAYR P, STAEVES J, SCHMOECKEL D. Deposition and investigation of TiN PVD coatings on cast steel forming tools[J]. Surface and Coatings Technology, 1997, 94/95: 446–450.
- [2] KOHLSCHEEN J, STOCK H R, MAYR P. Substoichiometric titanium nitride coatings as machinable surfaces in ultraprecision cutting[J]. Surface and Coatings Technology, 1999, 120/121: 740–745.
- [3] PENG Zhi-jian, MIAO He-zhuo, QI Long-hao, YANG Si-ze, LIU Chi-zi. Hard and wear-resistant titanium nitride coatings for cemented carbide cutting tools by pulsed high energy density plasma[J]. Acta Materialia, 2003, 51: 3085–3094.
- [4] MITSUO A, UCHIDA S, NIHIRA N, IWAKI M. Improvement of high-temperature oxidation resistance of titanium nitride and titanium carbide films by aluminum ion implantation[J]. Surface and Coatings Technology, 1998, 103/104: 98–103.
- [5] OHNUMA H, NIHIRA N, MITSUO A, TOYODA K, KUBOTA K, AIZAWA T. Effect of aluminum concentration on friction and wear properties of titanium aluminum nitride films[J]. Surface and Coatings Technology, 2004, 177/178: 623–626.
- [6] SHUM P W, LI K Y, SHEN Y G. Improvement of high-speed turning performance of Ti-Al-N coatings by using a pretreatment of high-energy ion implantation[J]. Surface and Coatings Technology, 2005, 198: 414–419.
- [7] HARRIS S G, DOYLE E D, VLASVELD A C, DODDER P J. Dry cutting performance of partially filtered arc deposited titanium aluminium nitride coatings with various metal nitride base coatings[J]. Surface and Coatings Technology, 2001, 146/147: 305–311.
- [8] LI Ming-sheng, WANG Fu-hui, SHU Yong-hua, WU Wei-tao. High temperature oxidation of $(\text{Ti},\text{Al})\text{N}$ and $(\text{Ti},\text{Al},\text{Y})\text{N}$ coatings on a steel prepared by arc ion plating (AIP)[J]. Materials Science Forum, 2004, 461/464: 351–358.
- [9] DONOHUE L A, LEWIS D B, MÜNZ W D, STACK M M, LYON S B, WANG H W, RAFAJA D. The influence of low concentrations of chromium and yttrium on the oxidation behaviour, residual stress and corrosion performance of TiAlN hard coatings on steel substrates[J]. Vacuum, 1999, 55: 109–114.
- [10] HARRIS S G, DOYLE E D, VLASVELD A C, AUDY J, LONG J M, QUICK D. Influence of chromium content on the dry machining performance of cathodic arc evaporated TiAlN coatings[J]. Wear, 2003, 254: 185–194.
- [11] KUTSCHEJ K, FATEH N, MAYRHOFER P H, KATHREIN M, POLCIK P, MITTERER C. Comparative study of $\text{Ti}_{1-x}\text{Al}_x\text{N}$ coatings alloyed with Hf, Nb, and B[J]. Surface and Coatings Technology, 2005, 200: 113–117.

(Edited by LONG Huai-zhong)